

Plasma Polymerization-Modified Bacterial Polyhydroxybutyrate Nanofibrillar Scaffolds

Zeynep Karahaliloğlu,¹ Murat Demirbilek,¹ Mesut Şam,² Melike Erol-Demirbilek,³ Necdet Sağlam,¹ Emir Baki Denkbaş^{1,4}

¹Nanotechnology and Nanomedicine Division, Hacettepe University, Ankara 06800, Turkey

²Department of Biology, Aksaray University, Aksaray 68100, Turkey

³Aksaray University, School of Health, Aksaray 68100, Turkey

⁴Department of Chemistry, Biochemistry Division, Hacettepe University, Ankara 06800, Turkey

Correspondence to: E. B. Denkbaş (E-mail: denkbas@hacettepe.edu.tr)

ABSTRACT: The design and the development of novel scaffold materials for tissue engineering have attracted much interest in recent years. Especially, the prepared nanofibrillar scaffold materials from biocompatible and biodegradable polymers by electrospinning are promising materials to be used in biomedical applications. In this study, we propose to produce low-cost and cell-friendly bacterial electrospun PHB polymeric scaffolds by using *Alcaligenes eutrophus* DSM 545 strain to PHB production. The produced PHB was characterized by Nuclear Magnetic Resonance (NMR) and Fourier Transform Infrared Spectroscopy (FTIR). Nanofibrous scaffolds were fabricated via electrospinning method that has a fiber diameter approximately 700–800 nm. To investigate cell attachment, cell growth, and antioxidant enzyme activity on positively and negatively charged PHB scaffold, PHB surface was modified by plasma polymerization technique using polyethylene glycol (PEG) and ethylenediamine (EDA). According to the results of superoxide dismutase (SOD) activity study, PEG-modified nanofibrillar scaffolds indicated more cellular resistance against oxidative stress compared to the EDA modification. As can be seen in cell proliferation results, EDA modification enhanced the cell proliferation more than PEG modification, while PEG modification is better as compared with nonmodified scaffolds. In general, through plasma polymerization technique, surface modified nanofibrillar structures are effective substrates for cell attachment and outgrowth. © 2012 Wiley Periodicals, Inc. *J. Appl. Polym. Sci.* 000: 000–000, 2012

KEYWORDS: biocompatibility; biopolymers and renewable polymers; polyesters; nanofiber

Received 1 March 2011; accepted 18 July 2012; published online

DOI: 10.1002/app.38370

INTRODUCTION

Tissue engineering aims at healing the damaged tissues by using a compatible biomaterial alone or cellularized.¹ Therefore, the design and the development of new materials as scaffold have attracted much interest. A functional nanoscale scaffold for tissue engineering can be an ideal template for cells to grow and function. The material and degradation products have to be biocompatible and able to provide mechanical and functional support for the cells to survive and grow. Also the nanoscaffold has to be able to provide an appropriate environment for the control of cell–cell and nanoscaffold–cell interaction.²

Synthetic and natural polymers play an important role in tissue engineering. Among them, bacterial polyhydroxyalkanoates (PHAs) are promising materials for biomedical applications because of being natural, renewable, biodegradable, and biocompatible thermoplastics. Degradation products can be

resorbed in a normal metabolic pathway.³ Polyhydroxybutyrate (PHB) is the simplest and the most extensively studied member of PHA family. PHB is produced as energy storage material by limiting concentration of basic nutrient like nitrogen and phosphorus in the presence of an excess of a carbon source.⁴ Over than 300 species of bacteria synthesized these polymers, but “*Alcaligenes eutrophus*” bacterium is the typically used one in the committed study of PHA synthesis due to PHA accumulation over 90% for dry cell weight.⁵ PHB has a high degree of crystallinity, hydrophobic character and an integral crystal structure, which leads to a high melting temperature of 178°C, poor stiffness and brittleness.^{6,7} Therefore, the direct use of PHB is hampered and the surface properties of the scaffolds have been modified to eliminate these restricts.

In tissue engineering, the same methods were widely used to prepare polymeric scaffolds, such as solvent casting, particulate

leaching, gas foaming, freeze-drying, thermally induce phase separating, fiber bonding, melt-molding, and electrospinning.⁸

Electrospinning is an excellent method to produce porous, nanoscale materials for tissue engineering. The diameters of the produced polymeric fibers are in the range of from 3 nm to greater than 5 μm .⁹ On scaffolds prepared by electrospinning technique adsorbed more proteins due to high surface-area volume ratio property of nanofibers. This means more binding sites for adsorbed proteins and cell membrane receptors. While cells spread on flat surfaces, nanoscale roughness on the scaffold increases cell attachment, spreading, proliferation and synthesis of extra cellular matrix (ECM) components.^{10,11}

In tissue engineering applications, surface chemistry and topography are essential for the cell attachment and growth. Optimal surface, chemical and physical properties; in particular improvement of the adhesion strength can be attained by altering the surface functionality.¹² Plasma surface modification is an effective surface treatment technique for many biomaterials in tissue engineering¹³ and it can change the surface properties of normally inert materials such as polymers, metals. In this study, plasma polymerization technique was used to improve surface properties of PHB nanoscaffold. Therefore, one of the hydrophilic substances, low molecular weight polyethylene glycol was used to improve hydrophilic properties of PHB fibers. PEG is a polyether that is known for its exceptional blood and tissue compatibility.¹⁴ EDA contains two primary amine groups. It was used in the study to form positive charge on the scaffolds surface and investigate effects on cell proliferation and metabolic activity. The amine groups provide active sites through which other bioactive molecules such as RGD peptide sequence could be attached.¹⁵

Superoxide dismutase (SOD) (EC.1.15.1.1), which specifically catalyzed the dismutation of superoxide radicals (O_2^-) to hydrogen peroxide (H_2O_2) and oxygen, has indicated that O_2^- is a normal and common byproduct of an oxygen metabolism. There is an increasing evidence to support the conclusion that superoxide radicals play a major role in cellular injury, cell adhesion, mutagenesis, and many diseases. In all cases, SOD has been shown to protect the cells against the deleterious effects.¹⁶

In this presented study, PHB was produced by *Alcaligenes eutrophus*. PHB nanofibrillar scaffolds were prepared by electrospinning technique and their surfaces were modified with plasma polymerization in which EDA or PEG used. The potential use of these modified nanofibrillar scaffolds for tissue regeneration was evaluated *in vitro* with L-929 cell line. The cell proliferation, cell viability and SOD activity of the cells on these scaffolds were investigated.

MATERIALS AND METHODS

Materials

Poly [(R)-3-hydroxybutyrate], (PHB) was supplied in powder form by Fluka (Switzerland) and had average molecular weight (M_w) of 540,000 g/mol to be used as a reference material to compare with our own product. Chloroform was used as solvent and was obtained from Sigma (USA). Polyethylene glycol (Acros, Belgium, $M_w = 300$ Da) and ethylenediamine (Fluka, USA) were

used for the modification of PHB scaffolds. 3-(4, 5-Dimethylthiazol-2-yl)-2, 5-Diphenyl tetrazolium Bromide (MTT) was purchased from Aldrich (USA). The growth medium consisting of Dulbecco Modified Medium (DMEM), supplemented with fetal calf serum (FCS), penicillin–streptomycin and trypsin-EDTA were purchased from Biological Industries (Israel).

PHB Synthesis and Characterization

Alcaligenes eutrophus DSM 545 was used for PHB production. Cultivation of bacteria consisted of two stages: in the first stage, bacteria were grown in nitrogen-rich medium which contained 10 g/L glucose, 2 g/L yeast extract, 2 g/L pepton, 1 g/L K_2HPO_4 , 1 g/L KH_2PO_4 , 1 g/L $(\text{NH}_4)_2\text{SO}_4$, 0.05 g/L $\text{MgSO}_4 \cdot 7\text{H}_2\text{O}$.

The bacteria were harvested by centrifugation and washed in order to remove residual nitrogen. In the second stage, cells were cultivated in a synthetic medium containing: 20 g sucrose, 1.5 g/L KH_2PO_4 , 3 g/L Na_2HPO_4 , 0.2 g/L $\text{MgSO}_4 \cdot 7\text{H}_2\text{O}$, 0.01 g/L $\text{CaCl}_2 \cdot 2\text{H}_2\text{O}$ and trace element solution: 2 g/L $\text{FeSO}_4 \cdot 7\text{H}_2\text{O}$, 0.3 g/L H_3PO_4 , 0.2 g/L $\text{CoCl}_2 \cdot 6\text{H}_2\text{O}$, 0.03 g/L $\text{ZnSO}_4 \cdot 7\text{H}_2\text{O}$, 0.03 g/L $\text{MnCl}_2 \cdot 4\text{H}_2\text{O}$, 0.03 g/L $(\text{NH}_4)_6\text{Mo}_7\text{O}_{24} \cdot 4\text{H}_2\text{O}$, 0.03 g/L $\text{NiSO}_4 \cdot 7\text{H}_2\text{O}$, 0.01 g/L $\text{CuSO}_4 \cdot 5\text{H}_2\text{O}$. The organism was cultivated under rotational agitation at 150 rpm and 30°C for 48 h in a 500-mL Erlenmeyer flask containing 200 mL of media.

After fermentation, the cell broth was concentrated by centrifugation at $4000 \times g$ for 15 min at 25°C, washed twice with distilled water, and then stored at -80°C for overnight. After this procedure, PHB containing biomass was mixed with 5 mL hypochlorite solution and suspension was treated for 24 h at 37°C. The mixture was centrifuged at $4000 \times g$ for 10 min. Hypochlorite solution phase was removed with a pipette. PHB contained cell debris was washed with distilled water at $4000 \times g$ for 10 min. Cell debris was mixed with 5 mL chloroform for 1 h at 37°C. The clear polymer solution was recovered by centrifugation to remove the majority of the non-PHB cell material; this was followed by polishing filtration. Finally, pure PHB was obtained by nonsolvent precipitation and filtration.

The 400 MHz 1H NMR spectrum of PHB was obtained by using a Bruker model AC400 L NMR spectroscopy. A PHB solution was prepared by using CDCl_3 at a concentration of 2% (w/v). The spectra were recorded at 25°C with a pulse repetition time of 3 s.

The Fourier Transform Infrared (FTIR) spectra were recorded using the Thermo Scientific (Nicolet iS10) spectrophotometer. Infrared (IR) absorption spectra were collected in the range $400\text{--}5000\text{ cm}^{-1}$ at room temperature with a resolution of 1 cm^{-1} .

Preparation and Characterization of PHB Scaffolds

The nanofibrillar scaffolds were prepared by the electrospinning technique. 5% (w/v) PHB solution was prepared in chloroform at 60°C. The polymer solution was then delivered to a 20-gauge metal needle (OD = 0.91 mm) connected to a high-voltage power supply. A CZE1000R Spellman high voltage power supply was used to generate a fixed potential of 17 kV. The polymer solutions were delivered at 2 mL/h flow rate by using Goldman syringe pump. The distance between the tip of the syringe and collector was 15 cm.

The morphological appearance of the nanofibrillar scaffolds was observed by Scanning Electron Microscope (SEM) (ZEISS EVO 50 EP, Germany).

To investigate how the surface topography affected the cells cultured on the scaffolds, SEM was used. Therefore, the prepared electrospun nanofiber scaffolds were sterilized with 70% ethanol and UV light. The scaffolds were washed once with the culture medium were then placed in a 96-well plate. L929 cells were seeded on each sample and cultured for 7 days at 37°C. The cells on nanofibrillar scaffolds were fixed in 4% paraformaldehyde solution for light and electron microscopy for 15 min at 4°C. Then the scaffolds were rinsed twice with PBS. The samples were dried, coated with Au.

The chemical compositions of nonmodified and EDA and/or PEG plasma-modified PHB surfaces were determined by using an X-Ray Photoelectron Spectrometer (XPS) and an XPS (Thermo Scientific K-Alpha, USA) equipped with a monochromatized Al K α X-ray source (1486.6 eV). The pass energy of the analyzer was 50 eV for high resolution core level spectra and the beam spot was 400 μ m. Curve fitting of the spectra was performed with the Thermo Avantage v4.41 Software. A Shirley-type correction was applied to the background under all fitted peaks.

Mechanical analyses in terms of the tensile strength, E-modulus and elongation at break of the PHB nanofiber scaffolds was assessed using a Zwick/Z010 mechanical testing machine, cross-head speed was 2 mm/min and 100N load cell was used. The scaffolds were cut into a rectangular shape, 12-mm length and 6-mm width. Mechanical test values indicated the average of obtained six measurements.

Surface Modification of Nanofibrillar Scaffolds

PHB nanofibrillar scaffolds were modified by the radio frequency glow discharge (RFGD) plasma deposition technique. Plasma modification system (Vacuum, Praha) was equipped with a 13.56 MHz radio frequency generator. The plasma reactor was attached to a vacuum pump for evacuation of reactor gas. The reactor was fed with monomer tank and argon gas during the process. For the modification of the scaffolds, PEG and EDA were used. The scaffolds were placed onto a stereofoam support deployed in the middle of the electrodes with 1 cm spaces between each of species. The argon gas was passed through the reactor at 0.1 mbar pressure in order to sweep away any reactive species like oxygen and nitrogen. Subsequently, the reactor was fed with coating compounds and the glow discharge initiated at power of 30 W. The plasma process was lasted for 10 min and the argon gas was passed through the chamber again to sweep away any gaseous residue. The scaffolds were kept in vacuum for 10 min for the stabilization of modification.¹⁷

Surface Electrochemical Properties

Surface electrochemical properties of the modified and nonmodified PHB nanofiber scaffolds ($n = 3$) were determined by measuring electroosmotic rates and surface charge densities obtained from potentiometric titrations. The rate of electroosmosis, which determines the zeta potential, was measured on the scaffold itself, whereas the surface charge was found on a suspension in the presence of salt including NaCl.¹⁸

Cell Culture and Cell Seeding

Mouse, fibroblast-like cells (L929) were cultured as a monolayer in Dulbecco's modified Eagle's medium (DMEM; Sigma-Aldrich, USA) supplemented with 10% fetal bovine serum (FBS, BIO-CHROM, Germany), 1% L-glutamine (Invitrogen, USA), together with 100 units/mL penicillin (Invitrogen, USA) and 100 lg/mL

streptomycin (Invitrogen, USA). The medium was replaced once in every 3 days and the cultures were maintained at 37°C in a wet atmosphere containing 5% CO₂. When the cells reached 80% confluence, they were trypsinized with 0.25% trypsin containing 1 mM ethylenediaminetetraacetic acid (EDTA; Invitrogen, USA) and counted by a hemocytometer (Hausser Scientific, USA) prior to being used in the experiments.

The indirect cytotoxicity evaluation of the nonmodified and EDA- and PEG-modified bacterial PHB nanofiber scaffolds were conducted by adapting the ISO10993-5 standard test method (indirect cytotoxicity) and MTT (3-(4,5-dimethylthiazol-2-yl)-2,5-diphenyltetrazolium Bromide) test was used. The MTT assay is a simple colorimetric assay to measure cell cytotoxicity, proliferation, and is based on the fact that metabolically active cells interact with a tetrasolium salt in an MTT reagent to produce an insoluble formazan dye, which absorbs light at the wavelength of 570 nm. The intensity of the absorbance is proportional to the number of viable cells. The indirect cytotoxicity of the modified scaffolds was determined with L929 mouse fibroblast cells. The nanofiber scaffolds were prewashed with 70% ethanol for 30 min; then, washed with autoclaved phosphate buffer saline (PBS) a few times, and finally washed once with the culture medium. Scaffolds were incubated at 37°C in a fresh culture medium in different days to prepare the extraction media ($n = 4$). The extraction ratio was 0.2 g/mL. L929 were seeded in a 96-well tissue-culture polystyrene plate (TCPS; Corning, USA) at 7×10^3 cells/mL and incubated overnight. Afterwards, the medium was replaced with the extraction medium for each type of the specimens and the cells were further incubated. After 24 h, the extraction medium was removed. 100 μ L of fresh medium and 13 μ L of MTT solution (5 μ g/mL, diluted with RPMI 1640 without phenol red) were pipetted to the each well. Incubation was allowed for another 4 h in dark at 37°C. Mediums were removed and 100 μ L/well isopropanol-HCl (absolute isopropanol containing 0.04M HCl) solution was added to dissolve formazan crystals. The wells were read at 570 nm on ASYS Expert Plus ELISA reader and the percentage of the cell viability was calculated. The control cells viability was defined as 100%. The cell viability percentage was calculated according to the following equation:

$$\text{Cell viability (\%)} = [\text{OD } 570(\text{sample})/\text{OD } 570(\text{control})] \times 100$$

The OD570 (sample) represents the measurement from the wells treated with nonmodified, EDA- or PEG-modified scaffolds extract mediums, and the OD 570(control) represents the measurements from the wells treated cell culture medium only.¹⁹

Cell Proliferation

For the proliferation study, EDA- or PEG-modified and nonmodified bacterial PHB nanofiber scaffolds (circular discs; 10 mm in diameter) were put in empty wells of TCPS. The specimens were sterilized by 70% ethanol for 30 min, washed two times with PBS and then washed with culture medium a few times. 2×10^3 in 50 μ L medium L929 cells were seeded on the each scaffold and incubated for 1 h to attach on the scaffolds. Then 2 mL medium was pipetted to each well and incubated for 1, 5, 7, and 10 days. After the each time point, the cell attachment and proliferation were quantified by MTT assay. After the each time point, the scaffolds were rinsed with PBS two times to remove unattached cells prior to MTT assay. And then, 250 μ L MTT reagent was pipetted onto the scaffolds and incubated for 4 h in dark at 37°C. After 4 h,

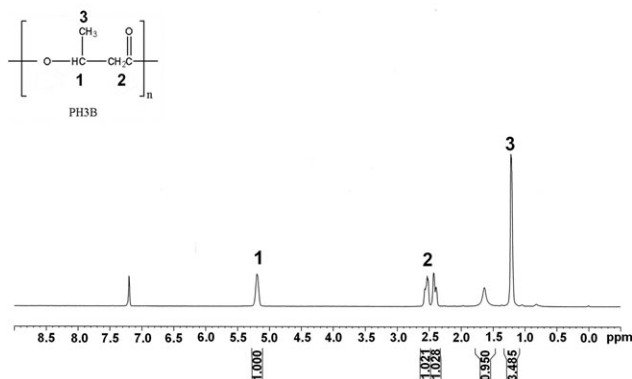


Figure 1. $^1\text{H-NMR}$ spectrum of bacterial poly[(R)-3-hydroxybutyrate] (PHB).

250 μL isopropanol-HCl solution was pipetted into the wells to dissolve formazan crystals. Then, dissolved formazan crystals were pipetted to 96-well plates and read at 570 nm on ASYS Expert Plus ELISA reader. The cell proliferation on the modified or non-modified scaffolds was assessed according to the formazan absorbances. Cell proliferation study was performed with the scaffold cells that were not seeded onto assess, cross-reaction the scaffolds, and MTT reagent. However, the absorbances were not noteworthy.

SOD Activity Assay

After 3, 10, and 15 days cultured L929 fibroblasts were detached from scaffolds with a trypsin-EDTA solution and protected at -80°C until the measurement of the SOD activities. Untreated L929 fibroblasts were used as the control group. SOD activity assay was performed according to the Yi-Sun's method.²⁰ Cells were homogenized in distilled water (1:10). 2.9 mL reaction mixture (40 mL of 3 mmol/L xanthine, 20 mL of 150 $\mu\text{mol/L}$ nitroblue tetrazolium (NBT), 12 mL of 400 mmol/L Na_2CO_3 and 6 mL of 1 g/L BSA), 50 μL supernatant and 50 μL xanthine oxi-

dase were mixed and incubated at room temperature for 20 min. After incubation, 1 mL 0.8 mM CuCl_2 were applied and monitored spectrophotometrically at 560 nm. One unit of SOD was defined as the amount of protein, which causes a 50% inhibition of the rate of NBT reduction. Protein contents were determined by the method of Lowry et al. using bovine serum albumin as the standard.²¹ Enzyme activities were expressed in U/mg protein.

Statistical Analysis

Statistical analysis was performed using the Statistical Package for the Social Sciences (SPSS) version 15 software. Statistical comparisons were made by analysis of variance (ANOVA). Scheffe's test was used for post hoc evaluations of the differences among groups.

RESULTS AND DISCUSSIONS

$^1\text{H-NMR}$ Composition Analysis

The $^1\text{H-NMR}$ spectra of the commercial PHB polymer has the characteristic signals of HB: ppm: the doublet at ca. 1.25 ppm is the side chain, a methyl group. The sextet at 5.25 ppm is the chiral carbon atom in the backbone with 5 vicinal hydrogens and near to the oxygen of the ester bond. The CH_2 in the backbone gives the signal at 2.5 ppm. The vicinal coupling of the proton resonance is due to the rotation of the $\text{CH}_2\text{-CH}$ backbone bond.²² Figure 1 shows the solid-state $^1\text{H-NMR}$ spectra of synthesized bacterial PHB from *Ralstonia eutropha* (*A. eutropha*). The NMR spectra of bacterial PHB consisted of three components like commercial PHB. When comparing NMR spectrum of bacterial with the commercial PHB, the characteristic peaks exhibited highly similar. These results implied that we synthesized high purity PHB from *Alcaligenes eutropha*.

FTIR Characterization

Characteristic bands for commercial PHB were at 1447 cm^{-1} corresponds to the asymmetrical deformation of the C—H bond in CH_2 groups and at 1380 cm^{-1} is the equivalent for CH_3 groups, at 1715 and 1278 cm^{-1} correspond to the stretching of

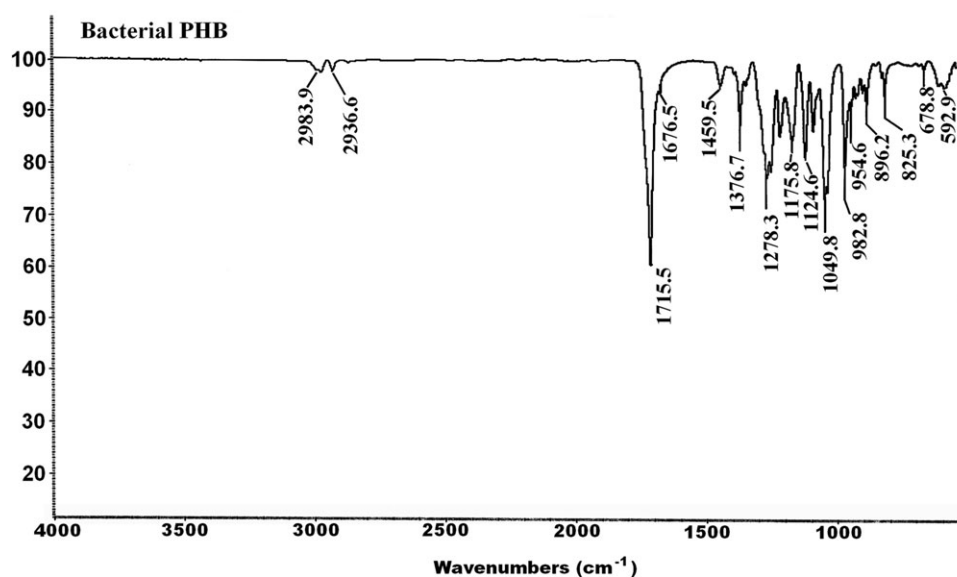


Figure 2. FT-IR spectrum of bacterial poly [(R)-3-hydroxybutyrate] (PHB).

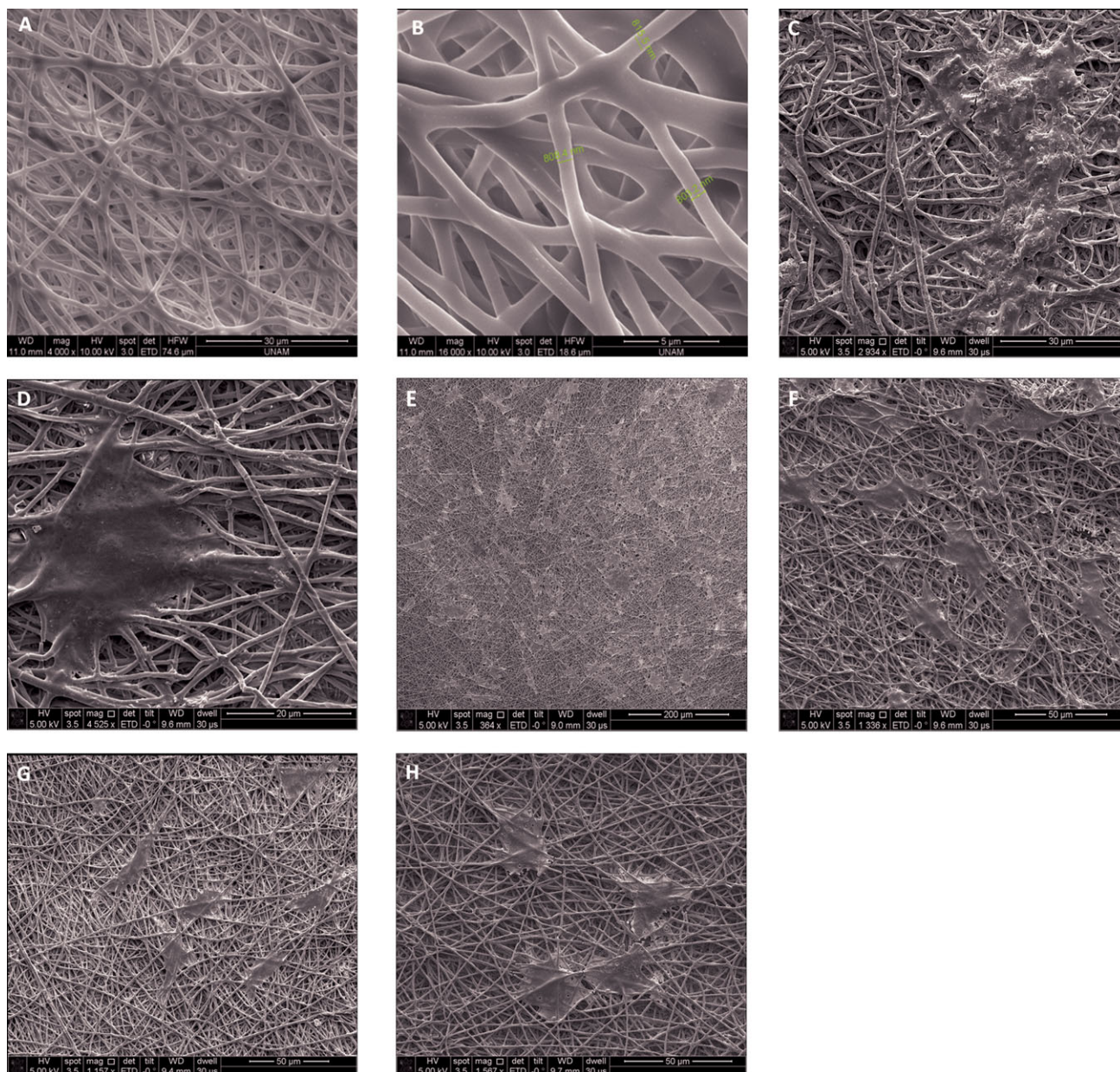


Figure 3. (A, B) SEM images of electrospun bacterial PHB nano fiber (prepared with 5% w/v PHB solution in chloroform with 25% v/v ethanol). Selected SEM images of L929 that were cultured (C, D) on non-modified, (E, F) EDA-modified, (G, H) PEG-modified PHB fibrous scaffolds for 7 day. [Color figure can be viewed in the online issue, which is available at wileyonlinelibrary.com.]

the C=O bond, whereas a series of intense bands located at 1000–1300 cm^{-1} correspond to the stretching of the C–O bond of the ester group. The IR spectrum of bacterial PHB is shown in Figure 2. Bacterial PHB had a strong adsorption band at 1278 cm^{-1} that is the characteristic for ester bonding. Other adsorption bands are at 1376, 1459, 2936, and 1715 cm^{-1} for $-\text{CH}_3$, $-\text{CH}_2$, $-\text{CH}$ groups respectively. The differences between band absorption for bacterial and commercial PHB were not found significant. All these bands are in full agreement with the observation of FTIR of commercial PHB. Additionally, the FTIR spectrum of both bacterial PHB and commercial PHB are close to the data given in the study of F.C. Oliveira et al. in 2007.²³

Electrospun of Bacterial PHB

In order to mimic a three-dimensional structure resembling that of a natural ECM, i.e., nanoscale fibrous network of collagens and proteoglycans, that promote the attachment, the

Table I. Mechanical Properties of the Nanofibrous PHB Scaffolds (Means \pm SD, $n = 6$)

	Tensile strength (MPa)	Elongation at break (%)
E-modulus (MPa)	2.01 \pm 0.43	2.53 \pm 0.37

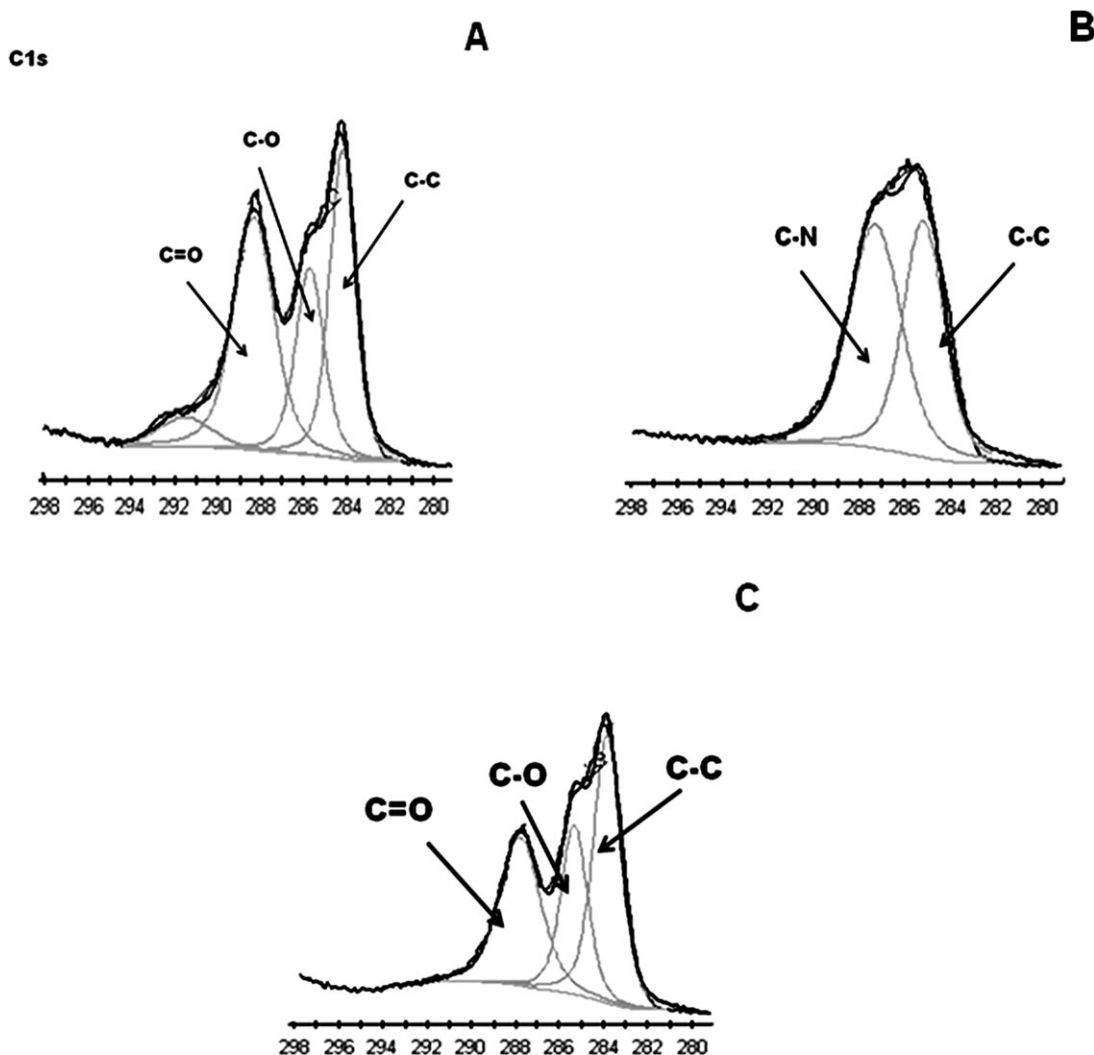


Figure 4. XPS C1s core-level spectra of: (A) nonmodified PHB; (B) EDA-PHB (EDA plasma-treated PHB); (C) PEG-PHB (PEG plasma-treated PHB).

proliferation, and the differentiation of the cells; electrospinning has been proven as a novel and effective method to produce such fibrous structures.

In this study, electrospun bacterial PHB scaffolds were fabricated from 5% w/v PHB solution in chloroform with an addition of 25% v/v ethanol. Figure 3(A, B) shows a selected SEM image of electrospun PHB fibers. Obviously, the individual fibers of the fiber mats are randomly oriented with large interconnected pores. Diameters of the individual fibers ranged between 700 and 800 nm, while the thickness of the fiber mats, after continuous electrospinning for 4 h.

Mechanical Properties

Mechanical properties of a scaffold are important aspects. Because of mechanical stability during the surgical period is required to repair an injured tissue. Table I summarized the mechanical integrity in terms of the tensile strength, E-modulus, and elongation at break of the PHB nanofibrous scaffolds. According to a study published by Suwantong et al. that the Young's modulus, tensile strength and elongation at break of prepared nanofiber matrix from commercial PHB is $147.3 \pm$

6.4 MPa , $1.6 \pm 0.06 \text{ MPa}$, and $2.3 \pm 0.7\%$. The mechanical properties of the both nanofibrillar scaffolds is fairly similarly when the mechanical test values of the above-mentioned nanofiber matrix is compared with the tensile properties of the bacterial PHB.²⁴

Plasma Modifications

Plasma-modified PHB nanoscaffolds were characterized with XPS system. Obtained results summarized in Figure 4 and Table II. They represent the C1s core-level spectra and surface elemental composition of PHB scaffolds, respectively. High-resolution scans of surfaces were taken at the C1s spectrum to determine the types of carbon species of the surfaces. The main peak at 284.22 eV of nonmodified PHB scaffolds attribute to hydrocarbons (C—C), the peak at 285.73 eV to ether carbon (C—O—), and the peak at 288.3 eV to carbonyl carbon (—C=O) [Figure 4(A)].²⁵

As for EDA-modified PHB scaffolds, nitrogen atom was incorporated on the surface which contributed to the C—N peak at 287.31 eV [Figure 4(B)]. The peak at 284.2 eV indicates C—C groups.

Table II. Surface Elemental Composition of non-modified and modified PHB scaffolds from C1s peak

Polymer	Atomic concentration (%)			C 1s peak fit (%)			
	C	O	N	C—C	C—N	C—O	C=C
PHB	65.89	31.15	-	32.28	-	22.12	39.22
EDA-PHB	47.51	19.2	31.81	30.85	37.38	-	-
PEG-PHB	57.43	40.07	-	39.87	-	24.16	32.78

Compared with nonmodified PHB, carbon and oxygen concentrations increase on PEG-modified scaffolds, which refers that new bonds were formed on the PEG-modified PHB surface due to plasma treatment [Figure 4(C)].

High-resolution C1s scans provided more precise information about PEG grafting to PHB scaffolds. The main carbon peak at 284 eV is the hydrocarbon or the C—C peak. The peak at a shift of 1.5 eV from the C—C peak is the carbonyl or the C—O peak (at 285.53 eV), a characteristic of PEG coupling.²⁶ The results were tabulated in Table II.

Surface Electrochemical Properties

According to results of surface charge densities and electroosmotic measurement, nonmodified scaffold surface charge density is 24 ± 3 mV; PEG-modified scaffold is 27 ± 5 mV and EDA-modified scaffold is $+87 \pm 9$ mV. These values indicates that surface modification of nanofiber membranes were performed successfully.

Indirect Cytotoxicity

Many researchers prefer indirect cytotoxicity method to assess material cytotoxicity.^{27–30} The method is a simple, effective ISO standard test. Harmful effects, originated from material on cells, such as degradation product, monomer or initiator residues, can be observed. In the study, to assess the cytotoxicity of plasma modification on L929 cells, indirect cytotoxicity method was used. To obtain extracts, the scaffolds were incubated with cell culture medium (0.2 g/mL) for 1, 5, 10, and 15 days and MTT test was used to observe the cytotoxic effects of the extracts. Indirect cytotoxicity results are summarized in Figure 5. According to the results, for all types of scaffolds, the

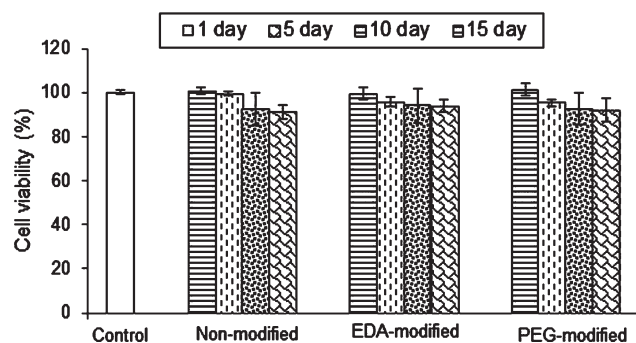


Figure 5. Indirect cytotoxicity of nonmodified, EDA or PEG modified bacterial PHB nanoscaffolds on L929 cell line ($n = 8$). The scaffolds were incubated in cell culture medium for 1, 5, 10, and 15 days. MTT test was used to assess the nanoscaffold extract cytotoxicity. The data is expressed as mean values (\pm standard deviation) of three separate experiments.

cytotoxicity rates increased, when the extraction times increased. Meanwhile, it was not seen statistically differences between non-modified, PEG- or EDA-modified by plasma polymerization and control for all day studies (at 15th day studies, $P = 0.945$ for nonmodified scaffolds, $P = 0.972$ for EDA-modified scaffolds, $P = 0.946$ for PEG-modified scaffolds). But, at 15th day studies; the following results were found; nonmodified PHB scaffold cytotoxicity rate is $8.92 \pm 3.31\%$; EDA-modified PHB scaffold cytotoxicity rate is $6.29 \pm 2.93\%$ and PEG-modified PHB scaffold cytotoxicity rate is 7.98 ± 5.56 . When compared EDA- and PEG-modification, it was not seen statistically differences ($P = 1.0$) between two types of modifications.

Cell Attachment and Cell Proliferation

To assess the attachment and the proliferation of L929 cells, they were cultured on the nanofibrous scaffolds for 1, 5, 7, and 10 days. The results are graphically shown in Figure 6. According to our results, at the 1st day of the studies, the formazan absorbance was found as 0.194 ± 6.74 for nonmodified scaffold; 0.238 ± 12.55 for EDA-modified scaffold and for PEG-modified scaffold, it was found as 0.248 ± 8.37 and it was not seen statistically differences between modified or nonmodified scaffolds ($P = 1.0$). For other days, it was found that the absorbances of the formazan products were increasing for all types of scaffolds. In the 5th day of the studies, it was observed that, the formazan absorbances obtained from EDA-modified scaffolds were more than the other type of scaffolds ($P < 0.05$). In addition, at 7th and 10th days formazan absorbances obtained from EDA-modified scaffolds were the highest amongst other types (Figure 6) ($P < 0.05$). When compared to the nonmodified scaffolds and modified scaffolds, the formazan absorbances were obtained less from nonmodified scaffolds for all day studies.

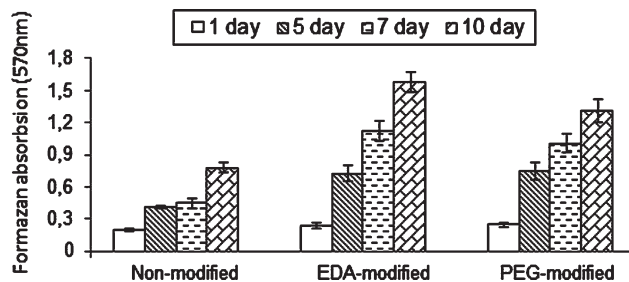


Figure 6. Cell proliferation on nonmodified, EDA or PEG modified bacterial PHB nanoscaffolds ($n = 8$). Totally, 2×10^3 cell/mL L929 cells were seeded onto the scaffolds. After the 1, 5, 7, and 10 days, MTT test was performed to obtain cell concentration on the scaffolds via formazan absorbance. The data is expressed as mean values (\pm standard deviation) of three separate experiments.

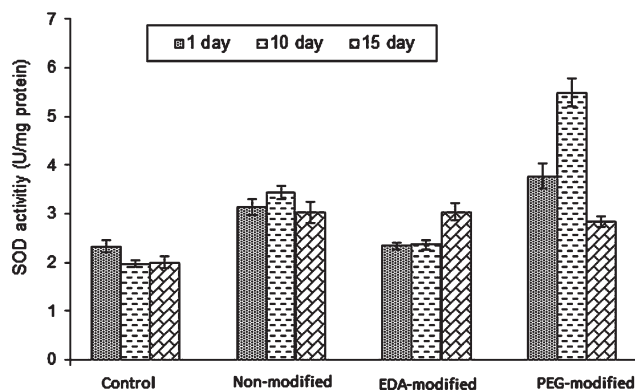


Figure 7. SOD activities of L929 cells cultured on modified and nonmodified scaffolds for 1, 10, and 15 days ($n = 8$). The data is expressed as mean values (\pm standard deviation) of three separate experiments.

The results indicate that, EDA- or PEG surface modification by plasma polymerization method leads to more cell attachment and cell proliferation.

Scanning Electron Microscope Studies

One of the important functions of the scaffolds is to support cell attachment and proliferation. To evaluate cellular behavior on the nanofibrous scaffolds as well as on EDA- or PEG-modified scaffolds with L929 cell, cells were seeded on the scaffolds and cultured for 7 days. After 7 days, the scaffolds were evaluated by SEM. Figure 3(C–H) shows the attachment of cells on both nonmodified and plasma-modified nanoscaffolds. The cells on EDA-modified scaffolds and also on PEG-modified scaffolds were significantly better than on nonmodified scaffolds. It indicates that plasma polymerization technique with EDA or PEG for surface modification is an effective method for cell attachment and outgrowth.

SOD Activity

A number of pathological damages such as carcinogenesis or cellular degeneration are due to reactive oxygen species (ROS). ROSs can be produced by sunlight, radiation, chemicals or metabolic processes. ROSs; such as superoxide radicals, are toxic to living cells since ROSs oxidize and degrade important biological macromolecules such as lipids and proteins. SOD catalyses the destruction of superoxide radicals and hence protects cells from the harmful effect of these free radicals.³¹ In the study, the SOD activity measurements were applied to observe any harmful effects resulted from bacterial PHB, PEG, or EDA modification. SOD activities of cells cultured on nonmodified, EDA or PEG-modified scaffolds were presented at Figure 7. Untreated cells were used as a control in the study. In the 3rd and the 5th day of the studies, it was observed that SOD activities of the cells cultured on all type of scaffolds increased ($p < 0.05$). But, a sharp increase was observed in SOD activity of the cells cultured on PEG-modified scaffold in the 5th day and it decreased rapidly ($p < 0.05$). In the 15th day of the studies, SOD activities were found less than they were found in the 3rd day ($p < 0.05$). Non-modified and PEG-modified scaffolds were caused to over production of superoxide radical on cells from the 3rd day to the 10th day ($p < 0.05$). Because of this, SOD activity was raised

as a cellular defense and in the 15th day, the activity was exhausted. Over production of superoxide radical may be the result from cell adhesion to scaffold or degradation product of PHB or excessive mitochondrial activity. It was clearly observed that maximum free radical production occurred in the cells treated on PEG-modified scaffold. For all day studies, it was found that SOD activities of control cells were the lowermost. When considering the cell proliferation and SOD activity studies, PEG or EDA modification, especially EDA modification caused more cell attachment and proliferation and the cells managed the harmful effects resulted from the bacterial PHB or EDA/PEG modification.

CONCLUSIONS

In this study, PHB, which was produced from *Alcaligenes eutrophus*, was purified and characterized. After that, PHB nanofiber scaffold was produced with the average fiber diameter, which was 700 nm, by electrospinning method. For the surface modification of electrospun PHB nanofiber scaffolds with EDA and PEG, plasma polymerization method was used. Adhesion and growth of L929 cells on PHB nanofibers were studied. Also indirect cytotoxicity test and SOD activities were performed to assess plasma polymerization with EDA or PEG cytotoxic effects. Especially, EDA modification was caused more cell attachment and cell proliferation. PEG modification was also increased the cell proliferation, but it's caused the SOD activities more than the others; especially it was seen at 10th day studies. The results indicate that, when compared the non-modified PHB nanoscaffold, surface modification by EDA or PEG was useful method for cell attachment and proliferation

ACKNOWLEDGMENTS

This study was carried out under the auspices of the Hacettepe University, Scientific Researches Unit. The authors would like to thank Koray Mizrak and Cem Bayram for their help in SEM and XPS characterizations.

REFERENCES

- Thire, R. M. S. M.; Meiga T. O.; Dick S.; Andrade L. R. *Macromol. Symp.* **2007**, *258*, 38.
- Gomes, M. E.; Reis, R. L. *Macromol. Biosci.* **2004**, *4*, 737.
- Lemoigne, M. *Bull. Soc. Chim. Biol.* **1926**, *8*, 770.
- Steinbuchel, A.; Valentin, H. E. *EMS Microbiol. Lett.* **1995**, *128*, 219.
- Schlegel, H. G.; Gottschalk, G.; von Bartta, R. *Nature (London)* **1961**, *191*, 463.
- Baptist, J. N. U.S. Patent 3044942 **1962**.
- Valappil, S. P.; Misra, S. K.; Boccaccini, A.; Roy, I. *Expert Rev Med Devices* **2006**, *3*, 853.
- Liu, X.; Ma, P.X. *Annals Biomed. Eng.* **2004**, *32*, 477.
- Subbiah, T.; Bhat, G. S.; Tock, R. W.; Pararneswaran, S.; Ramkumar, S. S. *J. Appl. Polym. Sci.* **2005**, *96*, 557.
- Agarwal, S.; Wendorf, J. H.; Greiner, A. *Polymer* **2008**, *49*, 5603.

11. Pattison, M. A.; Wurster, S.; Webster, T. J.; Haberstroh, K. M. *Biomaterials* **2005**, *26*, 2491.
12. Sodhi, R. N. S. *J. Electr. Spectrosc. Phenom.* **1996**, *81*, 269.
13. Chua, P. K.; Chena J. Y.; Wang L. P.; Huang N. *Mater. Sci. Eng.* **2002**, *R36*, 143.
14. Townsend, K. J.; Busse, K.; Kressler, J.; Scholz, C. *Biotechnol. Prog.* **2005**, *21*, 959.
15. Valuev, I. L.; Chupov, V. V.; Valuev, L. I. *Biomaterials* **1998**, *19*, 41.
16. Hassan, H. M. *Free Radic. Biol. Med.* **1988**, *5*, 377.
17. Aydin, H. M.; Turk, M.; Calimli, A.; Pişkin, E. *J. Artificial Organs* **2006**, *29*, 873.
18. Mullet, M.; Fievet, P.; Reggiani, J. C.; Pagetti, J. *J. Membr. Sci.* **1997**, *123*, 255.
19. Demirbilek, M. E.; Demirbilek, M.; Karahaliloğlu, Z.; Erdal, E.; Vural, T.; Yalçın, E.; Sağlam, N.; Denkbaş, E. B. *Appl. Biochem. Biotechnol.* **2011**, *164*, 780.
20. Yi-Sun, S.; Oberley, L. W.; Li, Y. *Clin. Chem.* **1988**, *34*, 497.
21. Lowry, O. H.; Rosebrough, N. J.; Farr, A. L.; Randall, R. J. *J. Biol. Biochem.* **1951**, *193*, 145.
22. Chiellini, E.; Gil, H.; Braunegg, G.; Burchert, J.; Gatenholm P.; van der Zee M. *Biorelated Polymers-Sustainable Polymer Science and Technology*; Eds. Springer-Verlag: Berlin Heidelberg, **2001**; p 147.
23. Oliveria, F. C.; Castilho, L. R.; Freire, D. M. G. *Bioresource Technol.* **2006**, *98*, 633.
24. Suwanton, O.; Waleetorncheepsawat, S.; Sanchavanakit, N.; Pavasant, P.; Cheepsunthorn, P.; Bunaprasert, T.; Supaphol, P. *Int. J. Biol. Macromol.* **2007**, *40*, 217.
25. Qu, X.; Wu, Q.; Liang, J.; Qu, X.; Wang, S.; Chen, G. *Biomaterials* **2005**, *26*, 6991.
26. Popat, K. C.; Sharma, S.; Desai, T. A. *J. Phys. Chem. B.* **2004**, *108*, 5185.
27. Dufrane, D.; Delloye, C.; Mckay, I. J.; De Aza, P. N.; De Aza, S.; Schneider, Y. J.; Anseau, M. *J. Mater. Sci.: Mater. Med.* **2003**, *14*, 33.
28. Lohbauer, U.; Jell, G.; Saravanapavan, P.; Jones, J. R.; Hench, L. L. *Key Eng. Mater.* **2005**, *284*, 431.
29. Buzzi, S.; Jin, K.; Uggowitz P. J.; Tosatti S.; Gerber I.; Loffler J. F. *Intermetallics* **2006**, *14*, 729.
30. Mattanavee, W.; Suwanton, O.; Puthong, S.; Bunaprasert, T.; Hoven, P. V.; Supaphol, P. *Am. Chem. Soc. Appl. Mater. Interfaces* **2009**, *1*, 1076.
31. Angelova, M.; Dolashka-Angelova, P.; Ivanova, E.; Serkedjieva, J.; Slokoska, L.; Pashova, S.; Toshkova, R.; Vassilev, S.; Simeonov, I.; Hartman, H.J.; Stoeva, S.; Weser, U.; Voelter, W. *Microbiology* **2001**, *147*, 1641.